Picard-Newton Iterative Method for Multimaterial Nonequilibrium Radiation Diffusion Problem on Distorted Quadrilateral Meshes

Jingyan Yue, Guangwei Yuan, Zhiqiang Sheng *

Abstract—**A new nonlinear iterative method for nonlinear parabolic equation is developed and applied to a multimaterial nonequilibrium radiation diffusion problem on distorted meshes. The new iterative method is named by Picard-Newton method (P-N for short). Solution process of the method is as follows. First, by linearizing the time-discretized nonlinear partial differential equation(PDE), we can get an iterative sequence of linear PDE. Then, we design the spatial discretization of the linear PDE, and educe a system of linear algebraic equations. Finally, solve the linear problem by Krylov-subspace methods. The main part of the method is consistent with Picard iterative method, and we can get P-N schemes by adding Newton correction terms to Picard scheme. The efficiencies of Picard method and Picard-Newton method are compared and the good performance of P-N method is demonstrated.**

Keywords: nonequilibrium radiation diffusion, Picard, Picard-Newton, nonlinear iterative method

1 Introduction

Many authors [1, 2, 3, 4, 5, 6] have studied the numerical solution of the nonequilibrium radiation diffusion equation coupled to a material energy equation. These equations are highly nonlinear and tightly coupled. It is pointed out that converging the nonlinearities within a time step may allow significantly larger time step sizes and improve accuracy as well [2, 3, 4]. Most researchers have used nonlinear Newton or Newton-Krylov solution techniques for these equations. A potential problem with Newton-type solution methods is that they can fail if the initial guess is not close enough to the converged solution. Simple iteration schemes (Picard-type method) can be more robust, but they are useful only if they converge fast enough.

This paper takes a different approach [8] to accelerate Picard iterative scheme that is easier to code into a computer program.The new method which is named by Picard-Newton method can be obtained from fully implicit Picard method by adding some Newton correction terms. It has some advantages of Picard method, e.g., its implementation is easy, and it gives a linear algebraic system with an explicit coefficient matrix. Furthermore, it can elicit certain iterative acceleration methods, which are faster than known methods such as the simpler Picard iteration.

The following section will present the equations as they are solved here. Section 3 introduces Picard-Newton iterative method. The test results are given in Section 4.

2 Description of the physical problem

The mathematical model employed in this manuscript is useful for applications in astrophysics and inertial confinement fusion. The equations for non-equilibrium diffusion coupled to material conduction are

$$\frac{\partial E}{\partial t} - \nabla \cdot (cD\nabla E) = c\sigma_a(aT^4 - E), \tag{1}$$

$$\rho C_v \frac{\partial T}{\partial t} - \nabla \cdot (\kappa \nabla T) = c\sigma_a(E - aT^4), \tag{2}$$

where E is the radiation energy density, t is the time, c is the speed of light, D is the radiation diffusion coefficient, σ_a is the photon absorption cross section, a is the Stefan-Boltzmann constant, T is the material temperature, ρ is the material density, C_V is the heat capacity, and κ is the material conduction coefficient.

To be consistent with previous works [6], these equations are nondimensionalized such that $\rho = C_v = c = a = 1$. With this nondimensionalization, the coupled radiation diffusion and material conduction equations are given by

$$\frac{\partial E}{\partial t} - \nabla \cdot (D\nabla E) = \sigma_a(T^4 - E), \tag{3}$$

*Laboratory of Computational Physics, Institute of Applied Physics and Computational Mathematics, Beijing 100088, P.R.China.The project is supported by the National Basic Research Program(2005CB321703), the National Natural Science Foundation of China (10501004), the Science Foundation of CAEP (2008B0202021, 2007B09008), the Foundation of National Key Laboratory of Computational Physics (9140C6902010805) and the Basic Research Project of National Defense (A1520070074).Email: yue_jingyan@iapcm.ac.cn

$$\frac{\partial T}{\partial t} - \nabla \cdot (\kappa \nabla T) = \sigma_a (E - T^4). \quad (4)$$

The energy exchange is controlled by the photon absorption cross section σ_a, which is modeled by

$$\sigma_a(T) = \frac{z^3}{T^3}.$$

In this model, z is a function of the material and varies as a function of space (x, y). High values of z and low values of T lead to higher energy exchange and therefore tighter coupling between equations (3) and (4).

The radiation diffusion coefficient without flux limiter is as follows:

$$D = \frac{1}{3\sigma_a}. \quad (5)$$

The material conduction coefficient (electron thermal conductivity of a fully ionized gas) κ has the following form

$$\kappa = c_0 T^{5/2}, \quad (6)$$

where $c_0 = 1.0 \times 10^{-2}$.

3 Picard-Newton iteration

In this section, we provide a detailed description of the proposed nonlinear iterative method. The solution process of Picard-Newton iterative method is as follows:

step 1 Linearize the time discretized nonlinear PDEs, and get a linear iteration sequence.

step 2 Design the spatial discretization of the resulting linear PDEs, and educe a system of linear algebraic equations.

step 3 Solve the linear problems by Krylov-subspace methods.

3.1 Newton linearization for the time discretized equations

Let

$$f_1 = \sigma_a(T^4 - E), f_2 = \sigma_a(E - T^4).$$

Consider the first-order time discretizations of the equations (3) and (4)

$$\begin{aligned} & F_1(E^{n+1}, T^{n+1}, \nabla E^{n+1}) \\ = \; & \frac{E^{n+1} - E^n}{\Delta t} - \nabla \cdot (D^{n+1} \nabla E^{n+1}) - f_1^{n+1} \\ = \; & 0, \end{aligned} \quad (7)$$

$$\begin{aligned} & F_2(E^{n+1}, T^{n+1}, \nabla E^{n+1}) \\ = \; & \frac{T^{n+1} - T^n}{\Delta t} - \nabla \cdot (\kappa^{n+1} \nabla T^{n+1}) - f_2^{n+1} \\ = \; & 0. \end{aligned} \quad (8)$$

Denote the grade by

$$\nabla E = (\nabla E_1, \nabla E_2)^T, \nabla T = (\nabla T_1, \nabla T_2)^T.$$

If equations (7) and (8) are linearized by one order Taylor expansion, and denote

$$\mathbf{A} = \begin{bmatrix} \frac{\partial \overset{(s)}{F}_1}{\partial E} & \frac{\partial \overset{(s)}{F}_1}{\partial T} & \frac{\partial \overset{(s)}{F}_1}{\partial \nabla E_1} & \frac{\partial \overset{(s)}{F}_1}{\partial \nabla E_2} & \frac{\partial \overset{(s)}{F}_1}{\partial \nabla T_1} & \frac{\partial \overset{(s)}{F}_1}{\partial \nabla T_2} \\ \frac{\partial \overset{(s)}{F}_2}{\partial E} & \frac{\partial \overset{(s)}{F}_2}{\partial T} & \frac{\partial \overset{(s)}{F}_2}{\partial \nabla E_1} & \frac{\partial \overset{(s)}{F}_2}{\partial \nabla E_2} & \frac{\partial \overset{(s)}{F}_2}{\partial \nabla T_1} & \frac{\partial \overset{(s)}{F}_2}{\partial \nabla T_2} \end{bmatrix},$$

$$\mathbf{U} = \begin{bmatrix} \overset{(s+1)}{E} - \overset{(s)}{E} \\ \overset{(s+1)}{T} - \overset{(s)}{T} \\ \nabla \overset{(s+1)}{E_1} - \nabla \overset{(s)}{E_1} \\ \nabla \overset{(s+1)}{E_2} - \nabla \overset{(s)}{E_2} \\ \nabla \overset{(s+1)}{T_1} - \nabla \overset{(s)}{T_1} \\ \nabla \overset{(s+1)}{T_2} - \nabla \overset{(s)}{T_2} \end{bmatrix},$$

we can get the following linear iteration sequence

$$\begin{bmatrix} \overset{(s)}{F}_1 \\ \overset{(s)}{F}_2 \end{bmatrix} - \mathbf{AU} = 0, \; s = 1, 2, \cdots, \quad (9)$$

where s is the nonlinear iteration index, and

$$\begin{aligned} \overset{(s)}{F}_1 = \; & \frac{E^{n+1,s} - E^n}{\Delta t} - \nabla \cdot (D^{n+1,s} \nabla E^{n+1,s}) \\ & - f_1^{n+1,s}, s = 1, 2, \cdots, \end{aligned}$$

$$\begin{aligned} \overset{(s)}{F}_2 = \; & \frac{T^{n+1,s} - T^n}{\Delta t} - \nabla \cdot (\kappa^{n+1,s} \nabla T^{n+1,s}) \\ & - f_2^{n+1,s}, s = 1, 2, \cdots. \end{aligned}$$

Note that the time level index, $n+1$, has been dropped. This is because the iteration is performed at the fixed time level $n+1$. Thus, we get a coupled linear PDE system

$$\begin{aligned} & \frac{\overset{(s+1)}{E} - E^n}{\Delta t} - \nabla \cdot (D(\overset{(s)}{T}) \nabla \overset{(s+1)}{E}) - f_1(\overset{(s)}{E}, \overset{(s)}{T}) \\ & - \nabla \cdot (D'_T(\overset{(s)}{T})(\overset{(s+1)}{T} - \overset{(s)}{T}) \nabla \overset{(s)}{E}) \\ & - \frac{\partial f_1(\overset{(s)}{E}, \overset{(s)}{T})}{\partial E}(\overset{(s+1)}{E} - \overset{(s)}{E}) \\ & - \frac{\partial f_1(\overset{(s)}{E}, \overset{(s)}{T})}{\partial T}(\overset{(s+1)}{T} - \overset{(s)}{T}) = 0, s = 1, 2, \cdots, \end{aligned} \quad (10)$$

$$\frac{\overset{(s+1)}{T}-T^n}{\Delta t}-\nabla\cdot(\kappa(\overset{(s)}{T})\nabla\overset{(s+1)}{T})-f_2(\overset{(s)}{E},\overset{(s)}{T})$$
$$-\nabla\cdot(\kappa'_T(\overset{(s)}{T})(\overset{(s+1)}{T}-\overset{(s)}{T})\nabla\overset{(s)}{T})$$
$$-\frac{\partial f_2(\overset{(s)}{E},\overset{(s)}{T})}{\partial E}(\overset{(s+1)}{E}-\overset{(s)}{E})$$
$$-\frac{\partial f_2(\overset{(s)}{E},\overset{(s)}{T})}{\partial T}(\overset{(s+1)}{T}-\overset{(s)}{T})=0, s=1,2,\cdots. \quad (11)$$

The resulting linear equations can preserve the parabolic property of original partial differential equations. For one dimensional nonlinear parabolic problem with Dirichlet boundary conditions, we can prove that as $s\to\propto$, the solution of the iterative sequence $\overset{(s)}{T}$ can converge to the solution of the time discretization equation, T^{n+1}, quadratically.

After designing spatial discrete scheme for the convection diffusion equations (10) and (11), we can get a Picard-Newton iterative scheme. Different spatial discrete scheme may correspond to different iterative scheme.

3.2 Spatial discretization of the linear iteration sequence on distorted meshes

Now, we introduce the spatial discretization scheme of the coupled linear PDE system. The first lines of equations (10) and (11) are consistent with Picard method, we need to consider the discretization of the Newton correction terms in addition. In this paper, we use a nine point scheme to discretize diffusion operator on distorted quadrilateral meshes [7]. Figure 1 shows the mesh stencil and some notations.

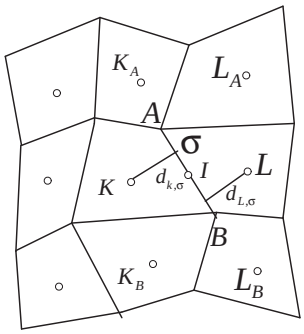

Figure 1: The mesh stencil and notation.

The discrete scheme of Eq. (10) on the cell K is

$$m(K)\frac{E_K^{n+1,s+1}-E_K^n}{\Delta t}$$
$$-\sum_{\sigma\in\partial K}\tau_\sigma^{n+1,s}(E_L^{n+1,s+1}-E_K^{n+1,s+1}$$
$$-D_\sigma(E_A^{n+1,s+1}-E_B^{n+1,s+1}))$$
$$-\sum_{\sigma\in\partial K}\mu_\sigma^{n+1,s}(T_\sigma^{n+1,s+1}-T_\sigma^{n+1,s})$$
$$(E_L^{n+1,s}-E_K^{n+1,s}-D_\sigma(E_A^{n+1,s}-E_B^{n+1,s}))$$
$$-((f_1)_K^{n+1,s}+\frac{\partial f_1}{\partial E}|_K^{n+1,s}(E_\sigma^{n+1,s+1}-E_\sigma^{n+1,s})$$
$$+\frac{\partial f_1}{\partial T}|_K^{n+1,s}(T_\sigma^{n+1,s+1}-T_\sigma^{n+1,s}))m(K)=0, \quad (12)$$

The discrete scheme of Eq. (11) on the cell K is analogous

$$m(K)\frac{T_K^{n+1,s+1}-T_K^n}{\Delta t}$$
$$-\sum_{\sigma\in\partial K}\overset{\sim}{\tau}_\sigma^{n+1,s}(T_L^{n+1,s+1}-T_K^{n+1,s+1}$$
$$-D_\sigma(T_A^{n+1,s+1}-T_B^{n+1,s+1}))$$
$$-\sum_{\sigma\in\partial K}\overset{\sim}{\mu}_\sigma^{n+1,s}(T_\sigma^{n+1,s+1}-T_\sigma^{n+1,s})$$
$$(T_L^{n+1,s}-T_K^{n+1,s}-D_\sigma(T_A^{n+1,s}-T_B^{n+1,s}))$$
$$-((f_2)_K^{n+1,s}+\frac{\partial f_2}{\partial E}|_K^{n+1,s}(E_\sigma^{n+1,s+1}-E_\sigma^{n+1,s})$$
$$+\frac{\partial f_2}{\partial T}|_K^{n+1,s}(T_\sigma^{n+1,s+1}-T_\sigma^{n+1,s}))m(K)=0, \quad (13)$$

where

$$\tau_\sigma^{n+1,s}=\frac{\tau_{K,\sigma}^{n+1,s}\tau_{L,\sigma}^{n+1,s}}{\tau_{K,\sigma}^{n+1,s}+\tau_{L,\sigma}^{n+1,s}}, \tau_{K,\sigma}^{n+1,s}=\frac{|AB|D_{K,\sigma}^{n+1,s}}{d_{K,\sigma}},$$

$$\mu_\sigma^{n+1,s}=\frac{\mu_{K,\sigma}^{n+1,s}\mu_{L,\sigma}^{n+1,s}}{\mu_{K,\sigma}^{n+1,s}+\mu_{L,\sigma}^{n+1,s}}, \mu_{K,\sigma}^{n+1,s}=\frac{|AB|\frac{\partial D_{K,\sigma}^{n+1,s}}{\partial T}}{d_{K,\sigma}},$$

$$\overset{\sim}{\tau}_\sigma^{n+1,s}=\frac{\overset{\sim}{\tau}_{K,\sigma}^{n+1,s}\overset{\sim}{\tau}_{L,\sigma}^{n+1,s}}{\overset{\sim}{\tau}_{K,\sigma}^{n+1,s}+\overset{\sim}{\tau}_{L,\sigma}^{n+1,s}}, \overset{\sim}{\tau}_{K,\sigma}^{n+1,s}=\frac{|AB|\kappa_{K,\sigma}^{n+1,s}}{d_{K,\sigma}},$$

$$\overset{\sim}{\mu}_\sigma^{n+1,s}=\frac{\overset{\sim}{\mu}_{K,\sigma}^{n+1,s}\overset{\sim}{\mu}_{L,\sigma}^{n+1,s}}{\overset{\sim}{\mu}_{K,\sigma}^{n+1,s}+\overset{\sim}{\mu}_{L,\sigma}^{n+1,s}}, \overset{\sim}{\mu}_{K,\sigma}^{n+1,s}=\frac{|AB|\frac{\partial\kappa_{K,\sigma}^{n+1,s}}{\partial T}}{d_{K,\sigma}},$$

$$D_\sigma=\frac{(L-K,A-B)}{|AB|^2},$$

$$D_{K,\sigma}=\frac{T_\sigma^3}{3z_K^3}, \kappa_{K,\sigma}=c_0T_\sigma^{5/2},$$

$$\frac{\partial D_{K,\sigma}}{\partial T}=\frac{T_\sigma^2}{z_K^3}, \frac{\partial\kappa_{K,\sigma}}{\partial T}=\frac{5}{2}c_0T_\sigma^{3/2},$$

$$E_\sigma=(E_A+E_B)/2, T_\sigma=(T_A+T_B)/2.$$

It's obvious that there are cell vertex unknowns in addition to cell-centered unknowns in the expression of discrete flux. We approximate the cell vertex unknowns by the cell-centered unknowns.

We have proposed some methods to eliminate the cell vertex unknowns in [7]. The expression of cell vertex unknowns is as follows:

$$u_p = \sum_{j=1}^{4} \omega_j u_{q_j},$$

where q_j is the center of cell around the cell vertex p, and ω_j is some combination coefficient.

P-N method can be obtained from fully implicit Picard method by adding Newton correction terms. It has some advantages of Picard method, e.g., its implementation is easy, and it gives a linear algebraic system with an explicit coefficient matrix. Furthermore, it can elicit certain iterative acceleration methods, which are faster than known methods such as the simpler Picard iteration.

4 Test problem

The test problem [6] is solved on the domain $\Omega = (0,1) \times (0,1)$. The value for z is 1 everywhere, except in the two obstacles defined by

$$\frac{3}{16} < x < \frac{7}{16}, \frac{9}{16} < y < \frac{13}{16}$$

and

$$\frac{9}{16} < x < \frac{13}{16}, \frac{3}{16} < y < \frac{7}{16},$$

where the value for z is 10. All four walls are insulated with respect to radiation diffusion and material conduction:

$$\left.\frac{\partial E}{\partial x}\right|_{x=0} = \left.\frac{\partial E}{\partial x}\right|_{x=1} = \left.\frac{\partial E}{\partial y}\right|_{y=0} = \left.\frac{\partial E}{\partial y}\right|_{y=1} = 0,$$

and

$$\left.\frac{\partial T}{\partial x}\right|_{x=0} = \left.\frac{\partial T}{\partial x}\right|_{x=1} = \left.\frac{\partial T}{\partial y}\right|_{y=0} = \left.\frac{\partial T}{\partial y}\right|_{y=1} = 0.$$

So the initial radiation spreads out and flows around the obstacles. The initial radiation energy is given by

$$E(r) = 0.001 + E_{amp} \exp\left[-\left(\frac{r}{0.1}\right)^2\right],$$

where r is the distance from the origin, which is located in the lower left corner of the computational domain:

$$r = \sqrt{x^2 + y^2}.$$

The initial material temperature is equal to the radiation temperature

$$T(x,y) = E(x,y)^{1/4}.$$

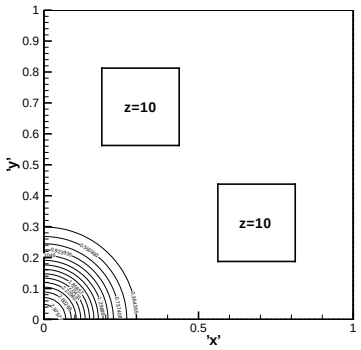

Figure 2: Initial conditions.

The initial conditions of this test problem are shown in figure 2.

In the following numerical experiments, we use two different meshes: uniform rectangular meshes, random quadrilateral meshes. Figure 3 shows random quadrilateral meshes, where the number of cells is 32×32. The edges of these obstacles correspond exactly to cell edges on these meshes, therefore, there are no mixed material cells.

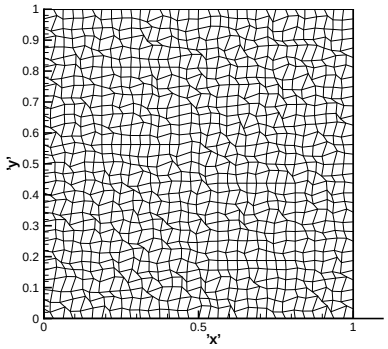

Figure 3: Random quadrilateral meshes.

GMRES is used as the linear solver, with the preconditioned ILUTP. The program is FORTRAN, and run on a windows system. The nonlinear convergence criterion is that the residual norm is less than 1.d-6 and relative residual norm is less than 1.d-2.

Table 1 respectively shows a mesh convergence study for Picard and P-N methods on rectangular meshes. In this study we cut the time step (dt) in half each time when the mesh spacing is cut in half. In Table 1 one can see that for both methods the number of nonlinear iterations per time step falls throughout the mesh refinement. Simultaneously, for P-N method, the number of GMRES iterations per nonlinear iteration is decreasing. While,

for Picard method, the number is fluctuant.

Table 1: Comparison of Picard and P-N methods for nonequilibrium radiation diffusion problem on rectangular meshes.

t=1.5	$\frac{Nonl.Its.}{dt}$	$\frac{Lin.Its.}{Nonl.}$	$\frac{Lin.Its.}{dt}$	con.error
Picard(64*64) dt=1.d-3	9.06	4.54	41.08	6.27d-8
P-N(64*64) dt=1.d-3	1.10	13.12	14.47	2.77d-9
Picard(96*96) dt=5.d-4	5.03	8.41	21.20	1.23d-7
P-N(96*96) dt=5.d-4	1.03	12.84	13.27	2.13d-8
Picard(128*128) dt=2.5d-4	3.52	5.81	20.42	2.54d-6
P-N(128*128) dt=5.d-4	1.00	11.55	11.57	4.83d-7

Table 2 shows a mesh convergence study on random quadrilateral meshes. For P-N method, the number of GMRES iterations per nonlinear iteration is approximately constant. For Picard method, the number of GMRES iterations increases throughout the mesh refinement. Figures 4 and 5 give the contours of radiation temperature of Picard and P-N methods on distorted meshes, respectively. We can see that the contours of P-N method accord with that of Picard method.

Table 2: Comparison of Picard and P-N methods for nonequilibrium radiation diffusion problem on random quadrilateral meshes.

t=1.5	$\frac{Nonl.Its.}{dt}$	$\frac{Lin.Its.}{Nonl.}$	$\frac{Lin.Its.}{dt}$	con.error
Picard(64*64) dt=1.d-3	9.02	5.24	47.31	4.65d-5
P-N(64*64) dt=1.d-3	1.14	15.32	17.40	4.69d-5
Picard(96*96) dt=5.d-4	5.03	6.57	33.08	2.37d-5
P-N(96*96) dt=5.d-4	1.05	15.79	16.65	2.32d-5
Picard(128*128) dt=2.5d-4	3.55	7.45	26.48	1.65d-5
P-N(128*128) dt=2.5d-4	1.01	15.02	15.21	1.40d-5

Table 1 and 2 give comparisons for linear iterations and nonlinear iterations between Picard and P-N methods. Since this test problem has reflecting boundary conditions, the total energy in the problem should be constant. Table 1 and 2 also provide conservation errors for Picard and P-N methods. From Table 1 and 2 the superiority of P-N method is clear.

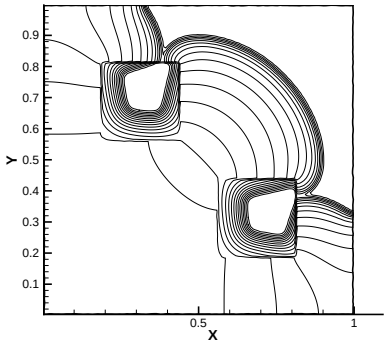

Figure 4: Final state radiation temperature on random quadrilateral meshes of Picard method.

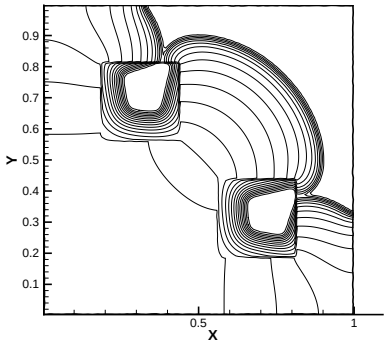

Figure 5: Final state radiation temperature on random quadrilateral meshes of P-N method.

5 Conclusions and Future Work

Picard-Newton method has some advantages of Picard method: its implementation is easy, and it gives a linear algebraic system with an explicit coefficient matrix. Furthermore, by adding Newton correction terms to Picard method, it can accelerate the convergence.

References

[1] D.A. Knoll, W.J. Rider, and G.L. Olson, "An efficient nonlinear solution method for non- equilibrium radiation diffusion", *J. Quant. Spectrosc. Radiat. Transfer*, 63:15-29, 1999.

[2] D.A. Knoll, W.J. Rider, G.L. Olson, "Nonlinear convergence, accuracy, and time step control in nonequilibrium radiation diffusion",*J. Quant. Spectrosc. Radia.*Transfer, 70 (2001), 25-36.

[3] D.A. Knoll, L. Chacon, L.G. Margolin, V.A. Mousseau, "On balanced approximations for time integration of multiple time scale systems",*Journal of Computational Physics,* 185 (2003), 583-611.

[4] V.A.Mousseau, D.A. Knoll, W.J. Rider, "Physics-Based Preconditioning and the Newton-Krylov Method for Non-equilibrium Radiation Diffusion", *J. Comput. Phys.* 160 (2000), 743-765.

[5] V.A. Mousseau and D.A. Knoll, "New physics-based preconditioning of implicit methods for non-equilibrium radiation diffusion",*J. Comput. Phys.*, 190:42-51,2003.

[6] V.A. Mousseau and D.A. Knoll, "Temporal Accuracy of the Nonequilibrium Radiation Diffusion Equations Applied to Two-Dimensional Multimaterial Simulations", *Nuclear Science and Enginerring*, 154:174-189, 2006.

[7] Zhiqing Sheng and Guangwei Yuan," A Nine Point Scheme for The Approximation of Diffusion Operators on Distorted Quadrilateral Meshes",*SIAM J. SCI. COMPUT.* Vol. 30, No. 3, pp. 1341-1361,2008.

[8] Guangwei Yuan,Xudeng-Hang, "Acceleration Methods of Nonlinear Iteration for Nonlinear Parabolic Equations",*J. Comput. Phys.* Vol.24, No.3, 2006.